THE JOURNAL OF PHYSICAL CHEMISTRY B

Article

pubs.acs.org/JPCB

Tunable Polymeric Sorbent Materials for Fractionation of Model Naphthenates

Mohamed H. Mohamed,[†] Lee D. Wilson,*[,‡] and John V. Headley[†]

[†]Water Science and Technology Directorate, Environment Canada, 11 Innovation Boulevard, Saskatoon, Saskatchewan, S7N 3H5, Canada

[‡]Department of Chemistry, University of Saskatchewan, 110 Science Place, Saskatoon, Saskatchewan, S7N 5C9, Canada

ABSTRACT: The sorption properties are reported for several examples of single-component carboxylic acids representing naphthenic acids (NAs) with β-cyclodextrin (β-CD) based polyurethane sorbents. Seven single-component examples of NAs were chosen with variable z values, carbon number, and chemical structure as follows: 2-hexyldecanoic acid (z = 0 and C = 16; **S1**), *n*-caprylic acid (z = 0 and C = 8; **S2**), *trans*-4-pentylcyclohexanecarboxylic acid (z = −2 and C = 12; **S3**), 4-methylcyclohexanecarboxylic acid (z = −2 and C = 8; **S4**), dicyclohexylacetic acid (z = −4; C = 14; **S5**), 4-pentylbicyclo[2.2.2]octane-1-carboxylic acid (z = −4; C = 14; **S6**), and lithocholic acid (z = −6; C = 24; **S7**). The copolymer sorbents were synthesized at three relative β-CD:diisocyanate mole ratios (i.e., 1:1, 1:2, and 1:3) using 4,4′-dicyclohexylmethane diisocyanate (CDI) and 4,4′-diphenylmethane diisocyanate (MDI). The sorption properties of the copolymer sorbents were characterized using equilibrium sorption isotherms in aqueous solution at pH 9.00 with electrospray ionization mass spectrometry. The equilibrium fraction of the unbound carboxylate anions was monitored in the aqueous phase. The sorption properties of the copolymer sorbents (i.e., Q_m) were obtained from the Sips isotherm model. The Q_m values generally decrease as the number of accessible β-CD inclusion sites in the copolymer framework decreases. The chemical structure of the adsorbates played an important role in their relative uptake, as evidenced by the adsorbate lipophilic surface area (LSA) and the involvement of hydrophobic effects. The copolymers exhibit molecular selective sorption of the single-component carboxylates in mixtures which suggests their application as sorbents for fractionation of mixtures of NAs. By comparison, granular activated carbon (GAC) and chitosan sorbents did not exhibit any significant molecular selective sorption relative to the copolymer materials; however, evidence of variable sorption capacity was observed among the sorbents investigated.

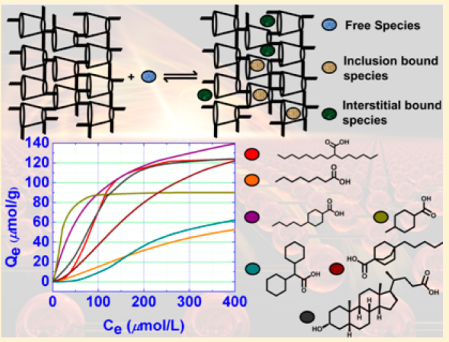

1. INTRODUCTION

Canadian oil sands deposits are vast and represent the second largest source of crude oil after Saudi Arabia for the North American economy.[1] The oil sands industry in Northern Alberta, Canada, employs a caustic warm water process, the Clark hot water extraction,[2] to extract oil sands. The resulting oil sands process water (OSPW) is saline and contains a complex mixture of organic compounds dominated by a class of naturally occurring naphthenic acids (NAs). The alkaline conditions solubilize NAs (cf. Scheme 1) as their naphthenate forms in aqueous solutions which are known to be toxic to aquatic organisms, algae, and mammals.[3−9] NAs are also suspected as endocrine-disrupting substances, however; the toxicology of the various component fractions of NAs is poorly understood at the present time.

NAs are recognized among the various toxic components in OSPW as a potential threat to human and ecosystem health, as outlined above. The structural formulas of NAs may be described by the conventional definition $C_nH_{2n+z}O_2$,[3,10−13] where "z" is referred to as the "hydrogen deficiency" and is a negative, even integer value. More than one isomer may exist for a given z value, with variable molecular weight, and the carboxylic acid group is generally attached to a side chain, rather than directly to the alicyclic ring.[9,10] The molecular weights differ by 14 amu (CH_2) between *n*-series and by 2 amu (2H) between z-series.[14] However, the term NAs has been widened recently to include other species containing multiple heteroatoms (i.e., O, N, and S), in addition to the traditional NAs (cf. Scheme 1). For example, OSPW is known to contain other components containing two or more carboxylic acids. Furthermore, O_x (x = 1−6) containing species along with NAs containing S- and N-heteroatoms are also present in the OSPW acid extractable fractions.[15]

The oil sands industry operates with a zero discharge policy where the OSPW is retained in vast tailing ponds. Given the estimated crude oil reserves (ca. 174 billion barrels bitumen) in the Athabasca oil sands and the significant water consumption (ca. 2−4 barrels of water per 1 barrel bitumen) for the extractive processing, there is growing interest to reclaim the OSPW to lower the industrial water footprint.[1] The estimated

Received: October 25, 2012
Revised: March 4, 2013
Published: March 7, 2013

   dx.doi.org/10.1021/jp310593p | *J. Phys. Chem. B* 2013, 117, 3659−3666

Scheme 1. Representative Structures of Naphthenic Acid Fraction Components (NAFC) in OSPW[a]

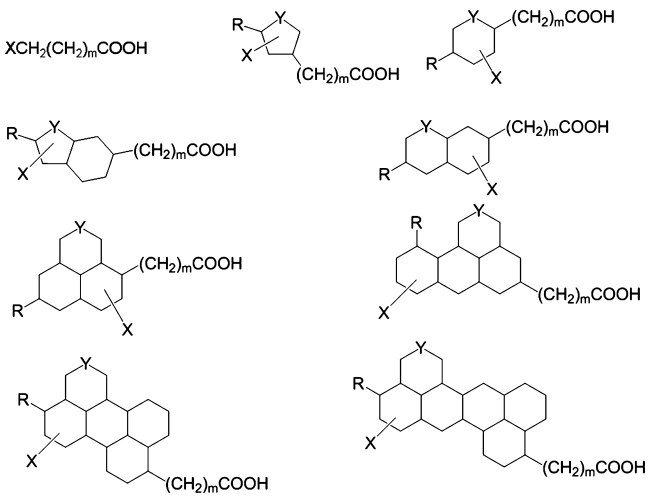

[a]R = alkyl group, X = COOH, R, OH, SO_x, NO_x, and SH, and Y = C, S, and N. The ring structures may not be fully saturated.

levels of NAs in the OSPW may be as high as 110 ppm, and despite the recycling of OSPW, residual levels of salts and NAs were reported to lead to corrosion problems.[6,16−18]

β-cyclodextrin (*β*-CD) based polyurethane copolymers were reported to have favorable sorption properties toward NAs in aqueous solution under alkaline conditions.[19,20] Molecular selective sorption toward the various molecular constituents in NAs with such types of copolymers is hypothesized according to the known variable binding affinity and sorption capacity in accordance with their relative cross-linker and cyclodextrin composition.[19−21] Thus far, no studies have been reported to evaluate this hypopthesis. Therefore, the objectives of this study are to investigate the potentiality of molecular selective sorption behavior of polyurethane sorbents containing *β*-CD toward NAs in aqueous solution. The two types of copolymers chosen for this study are copolymers prepared at *β*-CD:diisocyanate mole ratios (i.e., 1:1, 1:2, and 1:3) using 4,4′-dicyclohexylmethane diisocyanate (CDI) and 4′-diphenylmethane diisocyanate (MDI), respectively. Seven model naphthenate components were chosen with variable *z* values, carbon number, and chemical structure to represent examples of model NAs as follows: 2-hexyldecanoic acid ($z = 0$ and $C = 16$; **S1**), *n*-caprylic acid ($z = 0$ and $C = 8$; **S2**), *trans*-4-pentylcyclohexanecarboxylic acid ($z = -2$ and $C = 12$; **S3**), 4-methylcyclohexanecarboxylic acid ($z = -2$ and $C = 8$; **S4**), dicyclohexylacetic acid ($z = -4$; $C = 14$; **S5**), 4-pentylbicyclo[2.2.2]octane-1-carboxylic acid ($z = -4$; $C = 14$; **S6**), and lithocholic acid ($z = -6$; $C = 24$; **S7**).

2. EXPERIMENTAL SECTION

2.1. Materials. GAC (Norit Rox 0.8) and *β*-CD were purchased from VWR. 4,4′-Dicyclohexyl diisocyanate (CDI), 4,4′-diphenylmethane diisocyanate (MDI), dimethylacetamide (DMA), high molecular weight chitosan (150−375 kDa; ≥75% deacetylation), anhydrous ethyl ether, potassium bromide, 4 Å (8−12 mesh) molecular sieves, ammonium hydroxide, acetic acid, and formic acid were all purchased from Sigma Aldrich Canada Ltd. (Oakville, ON). Samples were stored in 2 mL HPLC amber vials with screw cap perforated Teflon-lined septa from Canadian Life Sciences. The carboxylic acids (**S1**−**S7**; cf. Figure 1) were purchased from Sigma Aldrich Canada Ltd. (Oakville, ON). Figure 1 illustrates the molecular structure of the individual components of NAs (**S1**−**S7**) investigated in this study.

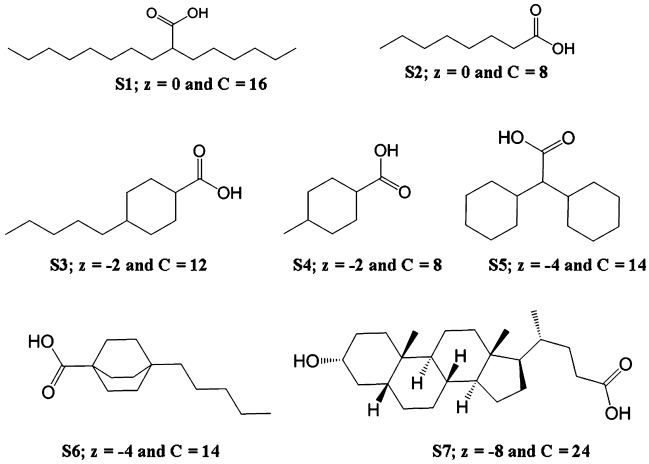

Figure 1. Molecular structure of the carboyxlic acids with variable *z* value, carbon number, and chemical structure: 2-hexyldecanoic acid ($z = 0$ and $C = 16$; **S1**), *n*-caprylic acid ($z = 0$ and $C = 8$; **S2**), *trans*-4-pentylcyclohexanecarboxylic acid ($z = -2$ and $C = 12$; **S3**), 4-methylcyclohexanecarboxylic acid ($z = -2$ and $C = 8$; **S4**), dicyclohexylacetic acid ($z = -4$; $C = 14$; **S5**), 4-pentylbicyclo[2.2.2]-octane-1-carboxylic acid ($z = -4$; $C = 14$; **S6**), and lithocholic acid ($z = -8$; $C = 24$; **S7**).

2.2. Synthesis and Characterization of Copolymer Materials. The nomenclature of the copolymers is described in accordance with the type of diisocyanate used and the relative comonomer mole ratio (*β*-CD/diisocyanate linker). For example, the 1:3 *β*-CD/CDI copolymer designation is referred to as **C*X*** (***X*** = 3), in which the molar quantity of *β*-CD in this designation is taken to be unity relative to 3 mol of CDI. **C*X*** and **M*X*** are the acronyms used hereafter for CDI and MDI, respectively. For example, in the case of 1:3 *β*-CD:CDI copolymer, the **C3** descriptor is applied and the mole content of *β*-CD is taken as unity for all copolymers. The synthesis of CD-based polyurethane materials was adapted from a previous report,[22] and the products were characterized with various spectroscopic, thermoanalytical, and elemental analysis methods.

2.3. Polymer Characterization. The IR spectra were obtained with a Bio-RAD FTS-40 instrument, and powdered samples were analyzed in reflectance mode. Samples were prepared by mixing ∼5 mg of copolymer with pure spectroscopic grade KBr (∼150 mg) by grinding in a mortar and pestle. DRIFT (diffuse reflectance infrared Fourier transform) spectra were recorded at room temperature with a resolution of 4 cm^{-1} over the range 400−4000 cm^{-1}. Fifty scans were recorded and corrected against a background spectrum of pure KBr. The DRIFT spectra are reported in Kubelka−Munk units, while the IR spectra of the neat liquids of HDI and CDI were obtained in transmittance mode using a sodium chloride sample cell.

^{1}H and ^{13}C NMR spectra in solution were acquired using a 500 MHz Bruker Avance NMR Spectrometer with an inverse triple resonance probe (TXI, 5 mm). Solid state ^{13}C NMR spectra were obtained with magic angle spinning (MAS) using a Varian Inova-500 operating at 125 MHz for ^{13}C nuclei.

dx.doi.org/10.1021/jp310593p | J. Phys. Chem. B 2013, 117, 3659−3666

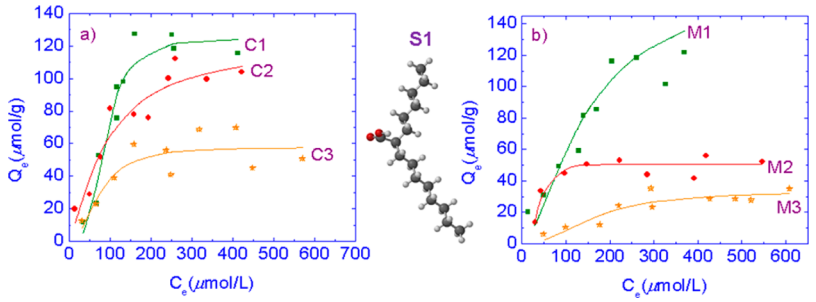

Figure 2. Equilibrium sorption isotherms for **S1** (see inset) and copolymer sorbents at pH 9.00 and 25 °C: (a) **C1**, **C2**, and **C3**; (b) **M1**, **M2**, and **M3**.

Samples were obtained with a MAS frequency of 16 kHz in 3.2 mm vespel rotors under $^{1}H \rightarrow {}^{13}C$ cross-polarization (CP) conditions with proton decoupling $\{^{1}H\}$ where chemical shifts referenced externally to adamantane (δ 38.5 ppm) at 295 K.

The elemental content (w/w, %) of carbon (C), hydrogen (H), and nitrogen (N) was measured by a Perkin-Elmer 2400 CHN Elemental Analyzer with a detection limit of ±0.3%. The results were uncorrected according to the estimated water/solvent content.

Thermal analyses of the copolymers were performed using a thermogravimetric analyzer, TGA (Q50 TA Instruments). Samples were heated in open aluminum pans to 30 °C and allowed to equilibrate for 5 min before further heating to 500 °C at a scan rate of 5 °C/min.

2.4. Sorption. Stock solutions of the carboxylic acids were prepared at variable concentration and pH 9.00 using 0.1 M ammonium hydroxide. The sorption experiments were maintained at pH 9.00 to ensure adequate solubility of the adsorbates.

To a 5 mL glass bottle with Teflon cap liners, ~10 mg of solid polymer was added to a fixed volume (4.00 mL) of an aqueous adsorbate solution with variable concentration ranging from ~10 to 100 mg/L. The vials were further sealed with parafilm between the cap and glass bottle and were incubated at room temperature in a horizontal shaker table to equilibrate for 24 h.

2.5. Mass Spectrometric Quantification. A Thermo-Scientific LTQ Orbitrap Velos mass spectrometer was used to monitor the degradation of the naphthenic acids. The spectrometer was operated with a 30 000 resolution setting. A full-scan mass spectrum was collected between m/z 100 and 600 using a lock mass of m/z 112.98563. Samples were quantified by extracting the mass range of the analyte of interest. For example, dicyclohexyl acetic acid (**S5**) was quantified by extraction of the mass range (m/z 223.16716−223.17398) and comparing the response area with a single point calibration standard made up to 100 mg L^{-1} for each component, respectively. The electrospray ionization (ESI) interface was set to negative ionization mode. Ionization with full scan MS conditions was optimized by calibrating the instrument and using automated tuning to optimize the transmission of m/z 112.98563. Parameters for the heated ESI interface (HESI) were as follows: source heater temperature, 53 °C; spray voltage, 2.86 kV; capillary temperature, 275 °C; sheath gas flow rate, 25 L h^{-1}; auxiliary gas flow rate, 5 L h^{-1}; spray current, 5.25 μA.

2.6. HPLC Separation. A Thermo-Scientific Accela 1250 pump equipped with a PAL auto sampler was utilized for the analysis. A mobile phase consisted of the following: solvent A, 90:10 water/CH_3CN; solvent B, 90:10 CH_3CN/water. Both solvents A and B contained 0.1% formic acid. The overall run time was 10:00 min. Initial conditions of 50% solvent A and 50% solvent B were changed linearly to 100% solvent B over a 5:00 min time period and then held at until 7:00 min before returning to initial conditions for a 3:00 min period to re-equilibrate the column step prior to the next injection. The analytical column was a 2.1 × 50 mm^2 Agilent Zorbax Eclipse Plus C_{18} (1.8 μm diameter particle size) which was maintained at 295 K. The flow rate was held constant at 200 μL min^{-1} throughout and resulted in variable retention times of **S1** 8.77 min, **S2** 2.25 min, **S3** 4.77 min, **S4** 1.56 min, **S5** 4.99 min, and **S6** 5.54 min, respectively. The injection volume was 5.00 μL.

2.7. Data Analysis. The sorption isotherms are represented as plots of the adsorbed amount of sorbate (S) from solution per unit mass of copolymer (Q_e) versus the unbound equilibrium concentration (C_e) of S in the aqueous solution. Equation 1 defines Q_e in relation to the experimental variables, C_0 is the initial stock concentration (M) of S, V is the volume of solution (L), and m is the mass of sorbent (g). It is important to note that the sorbents investigated herein are not soluble in aqueous solution.

$$Q_e = \frac{(C_0 - C_e) \times V}{m} \quad (1)$$

The Sips isotherm[23] (cf. eq 2) provides an assessment of the sorption parameters of the sorption process where the results may be interpreted in the context of the Langmuir or Freundlich models.[23,24] There are three adjustable parameters: Q_m (monolayer surface coverage), n_s (heterogeneity factor), and K_s (equilibrium constant).

$$Q_e = \frac{Q_m (K_s C_e)^{n_s}}{1 + (K_s C_e)^{n_s}} \quad (2)$$

The lipophilic surface area (LSA), volume ratio, and solvation energies of the apolar fragments of the carboxylic acids were calculated using Spartan '08 V1.2.0. The calculations were based on condensed-phase energy minimized molecular structures in water. Equilibrium geometries were obtained in the ground state with Hartree-Fock 3-21G.

3. RESULTS AND DISCUSSION

The characterization of the copolymer products was in agreement with previous results described elsewhere.[22]

Experimental isotherms are plotted as Q_e versus C_e, as shown in Figures 2−8 for carboxylic acids **S1**−**S7**. For these isotherms, the amount of sorbent was held constant (~10 mg), while the total concentration of the carboxylate anions varied between 10

dx.doi.org/10.1021/jp310593p | J. Phys. Chem. B 2013, 117, 3659−3666

Table 1. LSA, Dipole Moment, Free Energy of Solvation, and Q_m Values for Each Copolymer/Carboxylate System at 295 K

				Q_m (mg/g)					
carboxylate	LSA[a]	dipole moment[a] (D)	ΔG°_{solv} [a] (kJ/mol)	**C1**	**C2**	**C3**	**M1**	**M2**	**M3**
S1	327	5.99	−13.4	125	122	56.0	136	49.1	33.4
S2	170	2.33	−13.6	78.6	29.9	24.7	48.6	21.5	18.6
S3	222	6.43	−17.2	176	70.8	50.1	68.7	46.3	37.9
S4	143	6.27	−20.1	90.2	14.0	N/A	55.4	N/A	N/A
S5	233	5.24	−16.0	69.6	33.8	N/A	70.1	N/A	N/A
S6	240	2.34	−9.77	157	61.1	44.3	113	32.1	24.8
S7	357	2.15	−19.8	126	79.9	34.3	114	N/A	N/A

[a]Lipophilic surface area, dipole moments, and solvation energy values were obtained using Spartan '08 V1.2.0 from Hartree−Fock SCF calculation performed using Pulay DIIS + geometric direct minimization. The basis set used is 3-21G(*), and ΔG°_{solv} is the standard Gibbs energy of solvation.

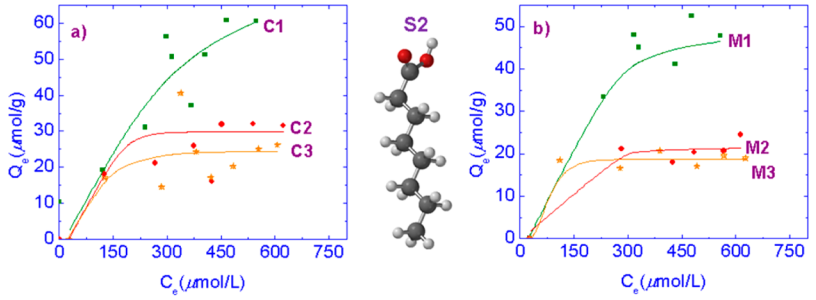

Figure 3. Equilibrium sorption isotherms for **S2** (see inset) and copolymer sorbents at pH 9.00 and 25 °C: (a) **C1**, **C2**, and **C3**; (b) **M1**, **M2**, and **M3**.

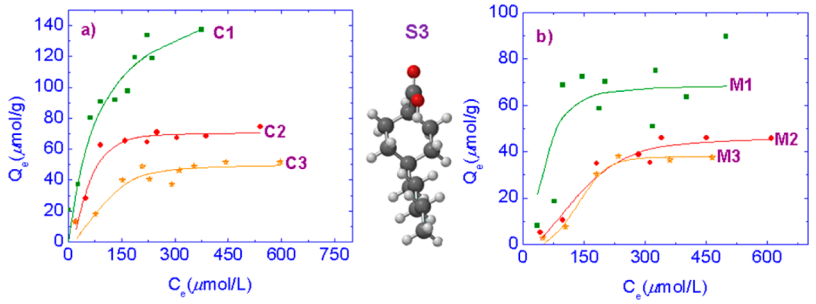

Figure 4. Equilibrium sorption isotherms for **S3** (see inset) and copolymer sorbents at pH 9.00 and 25 °C: (a) **C1**, **C2**, and **C3**; (b) **M1**, **M2**, and **M3**.

and 100 mg/L. In general, there is a monotonic increase observed for Q_e vs C_e as the total concentration (i.e., bound and unbound species) of carboxylate anion increases. The magnitude of Q_e for all carboxylate anions was found to decrease as the linker mole ratio increases. MDI-based copolymers display a reduced sorption capacity as compared with the CDI-based copolymers. This is due to the fact that the primary sorption takes place in the cavity sites of β-CD in the copolymers, as reported previously.[20,21] The Q_m values (cf. Table 1) were estimated from the "best-fit" according to the Sips model (cf. Equation 2) for each respective isotherm. Q_m reflects the sorption capacity of the monolayer according to the experimental conditions and varies with the molecular structure of the carboxylates and the sorbent, in accordance with the copolymer composition (i.e., 1:1, 1:2, and 1:3).

In the case of **S1** (cf. Figure 2), the magnitude of Q_e vs C_e is greatest for both copolymers with an equivalent mole ratio of β-CD and linker unit. However, a greater increase in Q_e observed for **C1** (cf. Figure 2a) is more evident than that for **M1** (cf. Figure 2b), indicating a favorable binding affinity of the former with **S1**. The isotherm **C2** (cf. Figure 1a) when compared to that of **M2** (cf. Figure 2b) shows a significant difference, where **M2** has a much lower value of Q_e which levels off at ∼150 μM. The saturation of the sorption sites is not observed for the 1:3 copolymers until the value of C_e extends beyond 250 μM for both materials.

According to a previous report,[25] **S2** (cf. Figure 3) was expected to display a reduced value of Q_e as compared with **S1**, due to its greater hydrophilic character (lower LSA) (cf. Table 1). The monotonic increase observed for Q_e with **S2** (cf. Figure 3) was more asymptotic, indicating an attenuated sorption affinity, as compared with **S1** (cf. Figure 2). Most of the isotherms reach saturation, as evidenced by the plateaus observed for all of the copolymers except for **C1** (cf. Figure 3a). In the case of the CDI copolymers, the isotherms reach saturation for **C2** and **C3** at ∼200 μM. In the case of the **M1** copolymer, the sorbent reaches saturation at ∼500−600 μM, whereas an earlier onset is observed for **M2** (300 μM) and **M3** (100 μM). Both **S1** and **S2** are saturated aliphatic carboxylates (i.e., z = 0) but differ according to the branching of the alkyl tail. The relative sorption affinity of **S1** appears to differ from **S2**, as evidenced by the different sorption capacities (i.e., **S1** >

dx.doi.org/10.1021/jp310593p | J. Phys. Chem. B 2013, 117, 3659−3666

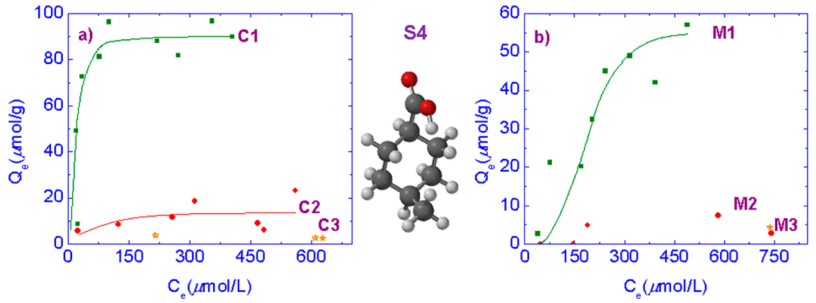

Figure 5. Equilibrium sorption isotherms for **S4** (see inset) and copolymer sorbents at pH 9.00 and 25 °C using (a) **C1**, **C2**, and **C3** and (b) **M1**, **M2**, and **M3**.

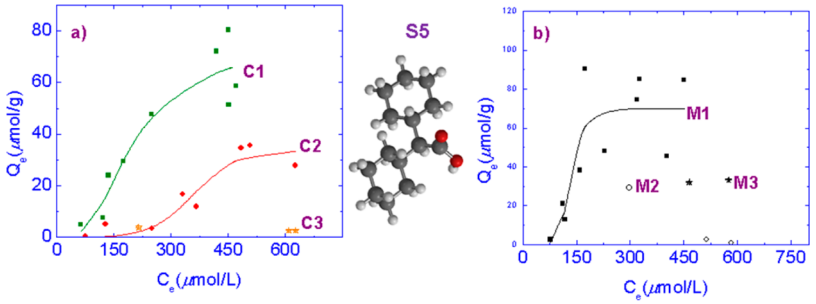

Figure 6. Equilibrium sorption isotherms for **S5** (see inset) and copolymer sorbents at pH 9.00 and 25 °C using (a) **C1**, **C2**, and **C3** and (b) **M1**, **M2**, and **M3**.

S2), in accordance with the relative apolar character of each sorbate (cf. Table 1). This affirms the previous conclusion that the apolar cavity of β-cyclodextrin plays a primary role in sorption as compared with the cross-linker domains of the copolymer framework.

S3 (cf. Figure 4) reveals a different pattern of the sorption behavior when compared to **S1** and **S2** in the presence of the **C1** copolymer. In general, the sorption capacity generally increases as the LSA of the carboxylate increases. In the case of **S3** (cf. Figure 4), the **C1** copolymer has a greater sorption capacity with **S3** (176 μM) as compared with **S1** (125 μM), despite the relative differences in LSA for each adsorbate. The sorption behavior for the other copolymers toward **S3** show a similar trend as observed for **S1** and **S2**. In the case of **C1**, saturation of the isotherm is not observed, whereas saturation occurs at ~200 μM for both **C2** and **C3**. Similarly, saturation of the MDI copolymers is observed for $C_e \sim 200$ μM.

The positive correlation between sorption affinity and the LSA of the sorbates is further observed for the sorption of **S4** (cf. Figure 5) when compared with **S3**. **S3** has a hydrocarbon chain and ring subunit, while **S4** solely contains a ring fragment (cf. Figure 5). Therefore, **S4** has a reduced LSA (cf. Table 1) relative to **S3**, where the relative sorption is attenuated for the former, as evidenced by the Q_m values in Table 1. Saturation of the sorption sites of the CDI copolymers is observed at $C_e \sim 80$ μM for both **C1** and **C2**, whereas **C3** showed minimal sorption. **C1** revealed a sharp increase for the uptake of **S4** prior to the plateau region of the isotherm, which indicates a stronger binding affinity for this carboxylate anion. These results provide further support that the linker framework adopts a secondary role in the sorption of the carboxylate anion and/or contributes to variation of the sorbent surface area.[25] The role of the linker framework has been shown previously where copolymers containing aliphatic cross-linker units (e.g., CDI) exhibit swelling of the framework due to water uptake, resulting in an increase of the apparent sorbent surface area.[26] In the case of copolymers with an aromatic cross-linker unit (e.g., MDI), limited swelling occurs due to the rigid nature of the copolymer framework. Furthermore, the secondary role of the linker framework sites was concluded to contribute to a lesser extent, but the relative contributions of these noninclusion sites are strongly dependent on the relative concentration of NAs.[20] In the case of the MDI copolymer, the sorption of **S4** was observed primarily for **M1**, whereas **M2** and **M3** display minimal sorption with **M1**. Saturation of the isotherm in the case of **M1** was observed at $C_e \sim 500$ μM, and the concentration dependence of Q_e is more gradual compared to that of **C1**. The latter agrees with the reduced sorption affinity between **M1** and **S4**.

Evidence of steric effects is shown for the sorption of **S5** (cf. Figure 6) with the **C1** copolymer. The carboxylic acid has a greater LSA compared to **S2**, **S3**, and **S4**; however, **S5** displays the lowest sorption capacity (cf. Table 1). This inverse relationship between Q_m and LSA is likely related to steric effects where a single ring unit of the sorbate is included within the inclusion site of β-CD for the **C1** copolymer. The isotherm concentration dependence of **S5** exhibits more variance as compared with the isotherms for other sorbates (i.e., **S1** and **S3**), indicating a reduced sorption affinity or factors associated with optimal ion formation during analyses. Evidence of attenuated sorption of **S5** with the copolymers is illustrated for the 1:2 and 1:3 copolymers (i.e., both CDI and MDI) where greater cross-linking attenuates the accessibility of the β-CD inclusion sites. These results support that the β-CD inclusion sites of the copolymer framework play a primary role in the sorption of the carboxylates. Greater cross-linking ratios (e.g., 1:3 copolymers) exhibit the greatest attenuation of the inclusion site accessibility of β-CD.[27]

The sorption affinity of the copolymers was observed to be greater for **S6** (cf. Figure 7) when compared with **S5** despite

dx.doi.org/10.1021/jp310593p | J. Phys. Chem. B 2013, 117, 3659−3666

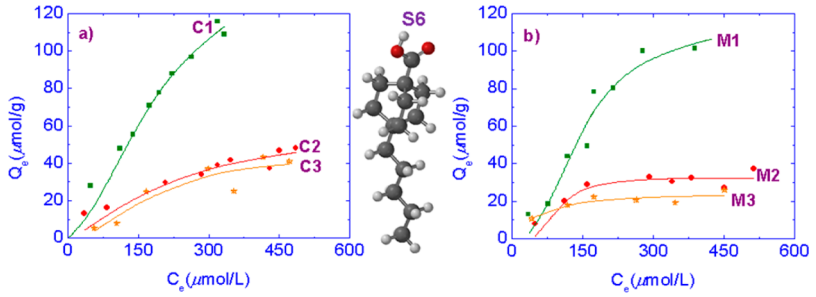

Figure 7. Equilibrium sorption isotherms for **S6** (see inset) and copolymer sorbents at pH 9.00 and 25 °C: (a) **C1**, **C2**, and **C3**; (b) **M1**, **M2**, and **M3**.

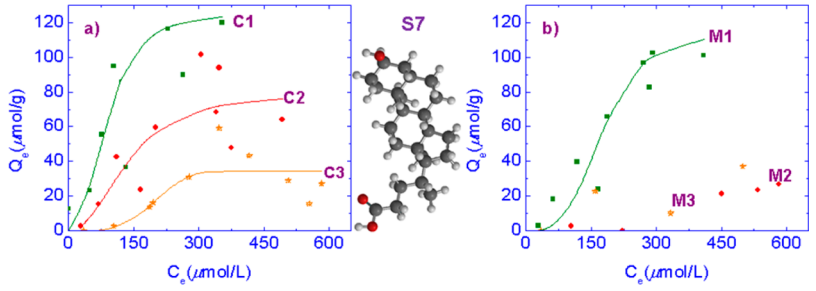

Figure 8. Equilibrium sorption isotherms for **S7** (see inset) and copolymer sorbents at pH 9.00 and 25 °C: (a) **C1**, **C2**, and **C3**; (b) **M1**, **M2**, and **M3**.

the comparative similarities of these species according to their *z*-values and carbon number. The LSAs of **S5** and **S6** are similar, whereas that of **S6** is slightly greater by ∼7 Å^2. The isotherm for **C1** does not show evidence of isotherm saturation, indicating the greater availability of potential sorption sites for the uptake of **S6**. However, there is a reduced slope for the **C1**/**S6** system when compared to **C1** with either **S1**, **S2**, **S3**, or **S4**, respectively. The results indicate that the **C1**/**S6** system has a reduced sorption affinity relative to the **S1**−**S4** adsorbate series. **S3** is structurally similar to **S6** except that the LSA is attenuated due to the presence of the additional cyclohexane ring of **S6**. Despite the greater LSA of **S6**, the uptake of this sorbate by the CDI-based copolymers is reduced and is attributed to attenuation of the sorption affinity resulting from steric effects. The sorption of **S6** with **C2** or **C3** revealed signs of isotherm saturation above 500 μM. In the case of MDI copolymers, the 1:1 copolymer showed relatively high sorption capacity toward **S6** when compared to **S3**. An opposite trend was observed for **C1**, and the effect of steric hindrance is not evident. The latter may be attributed to the role of the linker framework in addition to the β-CD inclusion sites for the sorption of the adsorbate. Similar to the results for **S1**, the sorption capacity of the MDI-based copolymers with **S6** decreases significantly, 1:2 (72%) and 1:3 (78%), as compared with the sorption properties of **M1**. The above results indicate the primary role of the β-CD inclusion sites and the secondary role of the linker domains for the sorption of naphthenates, in agreement with a recent study.[20]

Figure 8 illustrates the sorption behavior of the CDI- and MDI-based copolymers with **S7**. This carboxylic acid has the largest LSA among the various sorbates studied herein. The greatest sorption capacity is observed for the **C1** and **M1** copolymers. This reaffirms that the sorption of the carboxylates with the copolymers is not solely dependent on the LSA of the sorbates. The plateau observed for **C1** is poorly defined and illustrates that saturation of the available sorption sites was not met for these experimental conditions. In the case of **C1** and **C3**, the plateau is observed at ∼500 and ∼300 μM, respectively. The MDI copolymers reveal a similar trend for **S4** and **S5**, wherein the 1:2 and 1:3 materials show minimal sorption, while the 1:1 copolymer is similar to **S4**. This observation infers that carboxylates without a hydrocarbon chain (e.g., **S4**, **S5**, and **S6**) have limited sorption with the **M2** and **M3** copolymers. The reduced inclusion accessibility of the β-CD inclusion sites for the 1:2 and 1:3 copolymers hinders the formation of inclusion complexes for carboxylates possessing cyclic ring units vs *n*-alkyl chains (cf. Figure 1). In general, the CDI-based copolymers have greater sorption relative to MDI-based copolymers due to their propensity to undergo swelling and concomitant increases in sorbent surface area in aqueous solution, as reported previously.[26]

To further understand the selectivity of the copolymers toward the various carboxylates typically found in OSPW field samples, a simulated mixture containing **S1**−**S6** was prepared at 100 mg/L and sorption studies were conducted using **C1** and **M1**, respectively. Figure 9 illustrates the level of sorptive uptake of individual carboxylate anions from the simulated mixture. As mentioned previously, the CDI-based copolymers display more favorable sorption relative to the MDI-based copolymers. The trends based on the sorption of single carboxylic acids (cf. Table 1) when compared with the ternary mixtures yield markedly different results. For example, the relative sorption capacity (Q_m; cf. Table 1) of the C1 copolymer for single-component NAs adopted the relative ordering **S3** > **S6** > **S1** > **S4** > **S2** > **S5**. By comparison, the relative sorption capacity (percent uptake) for the C1 copolymer with the ternary mixtures of NAs adopted the following order: **S1** > **S6** > **S5** > **S3** > **S4** > **S2**. The observed differences in the sorption of single-component vs multicomponent mixtures may be due to the occurrence of synergism and higher order equilibria, since it is known that ternary complexes between CDs and multiple guest molecules may form.[28] One such example is β-CD/

dx.doi.org/10.1021/jp310593p | J. Phys. Chem. B 2013, 117, 3659−3666

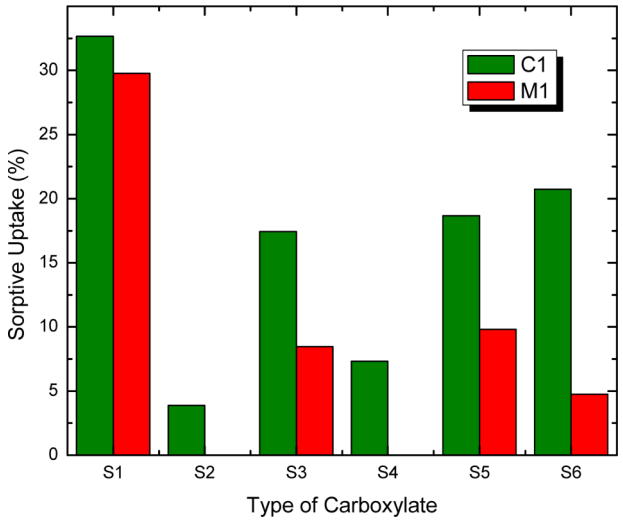

Figure 9. Percentage uptake of the individual carboxylates (**S1**−**S6**) from simulated ternary mixtures (100 mg/L of each component) using 10 mg of **C1** and **M1**, respectively.

pyrene/*n*-butanol, wherein the ternary complex is bound much more strongly than the binary complexes (i.e., CD/pyrene or CD/*n*-butanol). An additional factor which must be considered is the effect of activity coefficients and its role in modulating the apparent thermodynamic equilibrium constant.[29] The ternary complex for *β*-CD/pyrene/*n*-butanol can be understood in terms of the size−fit relationship of the host/guest(s) system, in addition to the solvent effects arising from the presence of the alcohol species. The latter is relevant to the importance of hydration and complex stability because the activity (a_i) of the solvent contributes significantly to the magnitude of the equilibrium binding constant of such host/guest complexes in aqueous solution.[30]

In addition to the *β*-CD-based copolymers, the sorption properties of GAC and chitosan were evaluated with the ternary mixtures of carboxylic acids. No apparent molecular selectivity was observed for these sorbents because all detectable amounts of carboxylates were adsorbed to a similar extent (results not shown).

4. CONCLUSIONS

In this sorption study, two types of copolymer sorbents containing variable levels of *β*-CD and cross-linker units were investigated to evaluate the molecular selective sorption of carboxylic acids representing NAs in OSPW samples. The specific examples of NAs vary according to their *z*-values and carbon number representing a range of adsorbates with variable size and LSA. The copolymers were observed to display molecular selective sorption behavior with carboxylate anions having variable size and LSA, in accordance with the tunable inclusion site accessibility of the copolymers. The copolymers described herein have two potential sorption sites where the *β*-CD inclusion sites exhibit the greatest affinity while the linker domains are secondary in nature. Different molecular profiles for the sorptive uptake of NAs were observed for the single-component and multicomponent mixtures. The results presented herein illustrate the potential application of cyclodextrin-based urethane sorbents for the fractionation of OSPW components into its constituent fractions. This sorbent technology will contribute significantly toward efforts in specialized remediation of aquatic environments containing OSPW and will contribute to QSAR studies of complex mixtures containing NAs.[31]

AUTHOR INFORMATION

Notes

The authors declare no competing financial interest.

ACKNOWLEDGMENTS

M.H.M. acknowledges the Natural Sciences and Engineering Research Council (NSERC) for the award of a Visiting Fellowship in a Canadian Government Laboratory. The authors gratefully acknowledge the University of Saskatchewan and Environment Canada for supporting this research. Mr. Jonathan Bailey and Mr. Kerry Peru are acknowledged for their expert technical assistance with the mass spectrometry measurements.

REFERENCES

(1) Nikiforuk, A. *Tar Sands: Dirty Oil and the Future of a Continent*; Greystone Books: Vancouver, BC, 2008.
(2) Chastko, P. A. *Developing Alberta's Oil Sands: From Karl Clark to Kyoto*; University of Calgary Press: Calgary, 2004.
(3) Wong, D. C. L.; van Compernolle, R.; Nowlin, J. G.; O'Neal, D. L.; Johnson, G. M. Use of Supercritical Fluid Extraction and Fast Ion Bombardment Mass Spectrometry to Identify Toxic Chemicals from a Refinery Effluent Adsorbed onto Granular Activated Carbon. *Chemosphere* **1996**, *32*, 1669−1679.
(4) Rogers, V. V.; Liber, K.; MacKinnon, M. D. Isolation and Characterization of Naphthenic Acids from Athabasca Oil Sands Tailings Pond Water. *Chemosphere* **2002**, *48*, 519−527.
(5) Headley, J. V.; Crosley, B.; Conly, F. M.; Quagraine, E. K. The Characterization and Distribution of Inorganic Chemicals in Tributary Waters of the Lower Athabasca River, Oilsands Region, Canada. *J. Environ. Sci. Health, Part A: Toxic/Hazard. Subst. Environ. Eng.* **2005**, *40*, 1−27.
(6) Quagraine, E. K.; Headley, J. V.; Peterson, H. G. Is Biodegradation of Bitumen a Source of Recalcitrant Naphthenic Acid Mixtures in Oil Sands Tailing Pond Waters? *J. Environ. Sci. Health, Part A: Toxic/Hazard. Subst. Environ. Eng.* **2005**, *40*, 671−684.
(7) Clemente, J. S.; Fedorak, P. M. A Review of the Occurrence, Analyses, Toxicity, and Biodegradation of Naphthenic Acids. *Chemosphere* **2005**, *60*, 585−600.
(8) Nero, V.; Farwell, A.; Lee, L. E. J.; Van Meer, T.; MacKinnon, M. D.; Dixon, D. G. The Effects of Salinity on Naphthenic Acid Toxicity to Yellow Perch: Gill and Liver Histopathology. *Ecotoxicol. Environ. Saf.* **2006**, *65*, 252−264.
(9) Peters, L. E.; MacKinnon, M.; Van Meer, T.; van den Heuvel, M. R.; Dixon, D. G. Effects of Oil Sands Process-affected Waters and Naphthenic Acids on Yellow Perch (Perca flavescens) and Japanese Medaka (Orizias latipes) Embryonic Development. *Chemosphere* **2007**, *67*, 2177−2183.
(10) Dzidic, I.; Somerville, A. C.; Raia, J. C.; Hart, H. V. Determination of Naphthenic Acids in California Crudes and Refinery Wastewaters by Fluoride Ion Chemical Ionization Mass Spectrometry. *Anal. Chem.* **1988**, *60*, 1318−1323.
(11) Fan, T. P. Characterization of Naphthenic Acids in Petroleum by Fast Atom Bombardment Mass Spectrometry. *Energy Fuels* **1991**, *5*, 371−375.
(12) St. John, W. P.; Rughani, J.; Green, S. A.; McGinnis, G. D. Analysis and Characterization of Naphthenic Acids by Gas Chromatography-Electron Impact Mass Spectrometry of Tert-butyldimethylsilyl Derivatives. *J. Chromatogr., A* **1998**, *807*, 241−251.
(13) Hsu, C. S.; Dechert, G. J.; Robbins, W. K.; Fukuda, E. K. Naphthenic Acids in Crude Oils Characterized by Mass Spectrometry. *Energy Fuels* **1999**, *14*, 217−223.
(14) Herman, D.; Fedorak, P. M.; MacKinnon, M. D.; Costerton, J. W. Biodegradation of Naphthenic Acids by Microbial Populations

Indigenous to Oil Sands Tailings. *Can. J. Microbiol.* **1994**, *40*, 467−477.
(15) Headley, J. V.; Peru, K. M.; Barrow, M. P. Mass Spectrometric Characterization of Naphthenic Acids in Environmental Samples: A Review. *Mass Spectrom. Rev.* **2009**, *28*, 121−134.
(16) Headley, J. V.; McMartin, D. W. A Review of the Occurrence and Fate of Naphthenic Acids in Aquatic Environments. *J. Environ. Sci. Health, Part A: Toxic/Hazard. Subst. Environ. Eng.* **2004**, *A39*, 1989−2010.
(17) Slavcheva, E. Review of Naphthenic Acid Corrosion in Oil Refining. *Br. Corros. J.* **1999**, *34*, 125−131.
(18) Turnbull, A.; Slavcheva, E.; Shone, B. Factors Controlling Naphthenic Acid Corrosion. *Corrosion* **1998**, *54*, 922−930.
(19) Mohamed, M. H.; Wilson, L. D.; Headley, J. V.; Peru, K. M. Novel Materials for Environmental Remediation of Tailing Pond Waters Containing Naphthenic Acids. *Process Saf. Environ. Prot.* **2008**, *86*, 237−243.
(20) Mohamed, M. H.; Wilson, L. D.; Headley, J. V.; Peru, K. M. Sequestration of Naphthenic Acids from Aqueous Solution using β-cyclodextrin-based Polyurethanes. *Phys. Chem. Chem. Phys.* **2011**, *13*, 1112−1122.
(21) Mohamed, M. H.; Wilson, L. D.; Headley, J. V.; Peru, K. M. Investigation of the Sorption Properties of β-cyclodextrin-based Polyurethanes with Phenolic Dyes and Naphthenates. *J. Colloid Interface Sci.* **2011**, *356*, 217−226.
(22) Mohamed, M. H.; Wilson, L. D.; Headley, J. V. Design and Characterization of Novel β-cyclodextrin Based Copolymer Materials. *Carbohydr. Res.* **2011**, *346*, 219−229.
(23) Sips, R. Structure of a Catalyst Surface. *J. Chem. Phys.* **1948**, *16*, 490−495.
(24) Freundlich, H. M. F. Over the Adsorption in Solution. *J. Phys. Chem.* **1906**, *57A*, 385−470.
(25) Mohamed, M. H.; Wilson, L. D.; Headley, J. V.; Peru, K. M. A Spectral Displacement Study of Cyclodextrin/Naphthenic Acids Inclusion Complexes. *Can. J. Chem.* **2009**, *87*, 1747−1756.
(26) Wilson, L. D.; Mohamed, M. H.; Headley, J. V. Surface Area and Pore Structure Properties of Urethane-Based Copolymers Containing β-cyclodextrin. *J. Colloid Interface Sci.* **2011**, *357*, 215−222.
(27) Mohamed, M. H.; Wilson, L. D.; Headley, J. V. Estimation of the Surface Accessible Inclusion Sites of β-Cyclodextrin Based Copolymer Materials. *Carbohydr. Polym.* **2010**, *80*, 186−196.
(28) Lin Peng, Y.; Te Wang, Y.; Wang, Y.; Jin, W. J. Current State of the Art in Cyclodextrin-Induced Room Temperature Phosphorescence in the Presence of Oxygen. *J. Photochem. Photobiol., A* **2005**, *173*, 301−308.
(29) Gelb, R. I.; Schwartz, L. M.; Cardelino, B.; Fuhrman, H. S.; Johnson, R. F.; Laufer, D. A. Binding Mechanisms in Cyclohexaamylose Complexes. *J. Am. Chem. Soc.* **1981**, *103*, 1750−1757.
(30) Gerasimowicz, W. V.; Wojcik, J. F. Azo Dye-α-Cyclodextrin Adduct Formation. *Bioorg. Chem.* **1982**, *11*, 420−427.
(31) Headley, J. V.; Peru, K. M.; Mohamed, M. H., Wilson, L. D.; McMartin, D. W.; Mapolelo, M. M.; Lobodin, V. V.; Rodgers, R. P.; Marshall, A. G., Electrospray Ionization Fourier Transform Ion Cyclotron Resonance Mass Spectrometry Characterization of Tunable Carbohydrate-Based Materials for Sorption of Oil Sands Naphthenic Acids. *Energy Fuels* [Online early access]. DOI: 10.1021/ef3014713. Published Online: Nov 25, **2012**.